Proceedings of the 7th International Conference on HydroScience and Engineering

Philadelphia, USA September 10-13, 2006 (ICHE 2006)

ISBN: 0977447405

Drexel University

College of Engineering

NUMERICAL SIMULATIONS OF FLOW AND SUSPENDED SEDIMENT TRANSPORT IN OPEN-CHANNEL FLOWS OVER SMOOTH-ROUGH BED STRIPS

Sung-Uk Choi[1], Moonhyeong Park[2], and Hyeongsik Kang[3]

ABSTRACT

The flow and transport of suspended sediment in open-channel flows over smooth-rough bed strips were simulated numerically. For the flow, the Reynolds-averaged Navier-Stokes equations were solved with the aid of the Reynolds stress model. Simulated mean flow structures are provided and compared with experimental data available in the literature. The sediment transport of suspended sediment in such flows was also simulated. The transport equation for suspended sediment was solved using the eddy diffusivity concept. The simulation resulted that the sediment concentration changes periodically in the transverse direction, showing higher concentration over the smooth strips. This is consistent with the previous field during the floods. The eddy diffusivity profile was also given and discussed.

1. INTRODUCTION

The existence of cellular secondary currents has been suggested by field observation first. Vanoni (1946) conjectured the presence of the cellular secondary currents from the periodic change in the lateral concentration of suspended sediment. Later, Kinoshita (1967), through aerial stereoscopic survey of a flood flow, noticed that high and low speed zones are repeated over the width and that the flows in the low speed zones are laden with high concentrations of sediment. Then, the cellular secondary currents were reproduced in the laboratory measurements through air duct experiments (Nezu and Nakagawa, 1984) and through open-channel experiments (Muller and Studerus, 1979; Wang and Cheng, 2005). Also, Nezu et al. (1993) presented field measurements of cellular secondary currents in a river in Japan using three component electro-magnetic flow meters.

Regarding the generation of the cellular secondary currents, no clear mechanism has been demonstrated so far. Two factors have been thought to be associated with initiating cellular secondary currents, i.e., the corner-induced vortices and the bottom sediment. However, through laboratory experiments, Nezu and Nakagawa (1989) observed that ridges and toughs are made at the middle part of the channel even before the ridge near the sidewall is not formed sufficiently. This implies that the role of the corner vortices is quite limited. Tsujimoto (1989) also found that the non-uniformity of bed particles contributes to generating or strengthening the cellular secondary

[1] Professor, School of Civil & Environmental Engineering, Yonsei University, Seoul 120-749, Korea (Tel: +82-02-2123-2797; Fax: +82-02-364-5300; schoi@yonsei.ac.kr); presently, Visiting Professor, Ralph M. Parsons Laboratory, Department of Civil & Environmental Engineering, Massachusetts Institute of Technology, USA
[2] Graduate Student, School of Civil & Environmental Engineering, Yonsei University, Seoul 120-749, Korea (liege@yonsei.ac.kr)
[3] Research Professor, School of Civil & Environmental Engineering, Yonsei University, Seoul 120-749, Korea (kanghs@yonsei.ac.kr)

currents. Colombini (1993) showed that the erodible bottom with uniform sediment is responsible for initiating mechanism of cellular secondary currents rather than corner vortices by the sidewalls. Subsequently, Colombini and Parker (1995) extended Colombini's (1993) work to non-uniform sediment case.

The purpose of the present paper was to simulate the flow structure and suspended sediment transport in open-channel flows over smooth-rough bed strips. For flow, the RANS (Reynolds-Averaged Navier-Stokes) equations were solved numerically with the Reynolds stress model for turbulence closure. For sediment transport, the transport equation of the suspended sediment was solved numerically. The eddy viscosity concept was used just for simplicity. The simulated mean flow and turbulence statistics were compared with experimental data, showing a good agreement. Hydraulic characteristics of simulated results of suspended sediment concentration were also discussed.

A numerical model, if it has to be used in investigating the generating mechanism of cellular secondary currents, should be equipped with a turbulence model that is capable of simulating the mean flow and turbulence statistics of such flows well. In addition, another turbulence model is required for predicting sediment transport. Then, the numerical model should handle the moving boundary of the bed that deforms by the sediment deposition or erosion. This will allow the formation of sand ridges and troughs for uniform sediment. In order to reproduce the transverse variation in roughness, the model should also deal with mixture of sediment. Additional incorporation of the moving boundary for the free surface will improve the prediction of flow structure. The present paper corresponds to the first stage of an application of RANS model and eddy diffusivity concept-based sediment transport model to flows over smooth-rough bed strips.

2. FLOW EQUATIONS

The continuity and momentum equations of the RANS model are given, respectively, by

$$\frac{\partial \overline{u_i}}{\partial x_i} = 0 \tag{1}$$

$$\frac{\partial \overline{u_i}}{\partial t} + \overline{u_j}\frac{\partial \overline{u_i}}{\partial x_j} = -\frac{1}{\rho}\frac{\partial \overline{p}}{\partial x_i} + \frac{\partial}{\partial x_j}\left(\nu \frac{\partial \overline{u_i}}{\partial x_j}\right) - \frac{\partial \overline{u_i' u_j'}}{\partial x_j} + g_i \tag{2}$$

where the mean and fluctuating velocity components are denoted by $\overline{u_i}$ and u_i' in the i-direction, respectively. In eq. 2, ρ is the fluid density, $\overline{p}$ is the mean pressure, ν is the kinematic viscosity, $-\overline{u_i' u_j'}$ denotes the Reynolds stress, and g_i is the gravitational acceleration.

2.1 Reynolds Stress Model

In the present study, the Reynolds stress model is used for the turbulence closure of the flow equations, eqs. 1 and 2. The Reynolds stress components R_{ij} (= $\overline{u_i' u_j'}$) in eq. 2 are obtained by solving the following transport equation for Reynolds stress:

$$\overline{u_k}\frac{\partial R_{ij}}{\partial x_k} = -\left(R_{ik}\frac{\partial \overline{u_j}}{\partial x_k} + R_{jk}\frac{\partial \overline{u_i}}{\partial x_k}\right) + D_{ij} - \varepsilon_{ij} + \Pi_{ij} \tag{3}$$

where D_{ij} is the transport of R_{ij} by diffusion, ε_{ij} the rate of dissipation of R_{ij}, and Π_{ij} the transport of R_{ij} due to turbulent pressure-strain interactions. Mellor and Herring's (1973) model, Speziale et al.'s (1991) model, and Hanjalic and Lauder's (1972) model are used for the turbulent diffusion term, the pressure-strain correlation term, and the dissipation rate term, respectively. The choice of these sub-models is based on numerical experiments reported by Choi and Kang (2001).

The free surface is treated as a symmetric plane for all dependent variables except for the dissipation rate of the turbulent kinetic energy (ε). For ε, the relationship by Naot and Rodi (1982) is prescribed at the free surface in order to increase the dissipation level of the turbulence kinetic energy. It is assumed that the flow at the node closest to the wall obeys the standard log-law. The log-law constant for rough walls is obtained from Naot and Emrani (1983). Since local equilibrium is assumed in the vicinity of the wall, the dissipation rate is set equal to the production of the turbulence kinetic energy. For the Reynolds normal stress at the wall, the zero gradient condition is used. The Reynolds shear stress in the vicinity of the wall is set equal to the value from the logarithmic law (Lin, 1990).

2.2 Equation for Suspended Sediment Transport

For a given flow field, the distribution of suspended sediment can be computed by solving the following mass conservation equation for suspended sediment:

$$\frac{\partial \bar{c}}{\partial t} + \frac{\partial}{\partial x_j}\left[\left(\overline{u_j} - w_s \delta_{j3}\right)\bar{c}\right] = \frac{\partial}{\partial x_j}\left(\frac{\nu_t}{\sigma_c}\frac{\partial \bar{c}}{\partial x_j}\right) \tag{4}$$

where $\bar{c}$ is the time-averaged mean concentration of suspended sediment, w_s is the fall velocity of the sediment particle, ν_t is the eddy viscosity, and σ_c is the turbulent Schmidt number relating the turbulent diffusivity of sediment particles to the eddy viscosity. In this study, a value of σ_c=1.0 is used and the terminal fall velocity is estimated from the relationship proposed by Dietrich (1982). For the computation of distributed suspended sediment, zero flux conditions are imposed at the free surface and sidewalls. The near-bed concentration at the equilibrium state from Garcia and Parker (1991) and zero flux condition are imposed on the smooth and rough strips, respectively.

3. MEAN FLOW STRUCTURE

The numerical model is applied to laboratory experiments performed by Wang and Cheng (2005). Wang and Cheng made periodically changing roughness by glueing particles (d_{50} = 2.55 mm) on the rough strips in a 0.6 m wide and 0.075 m deep channel. The width of the rough strips, same as that of smooth strips, was set to the flow depth. The resulting width-to-depth ratio is 8, and the channel slope was 0.0007. Wang and Cheng measured the velocity components u and w using the laser Doppler anemometer and estimated the component v using the continuity relationship.

Figure 1 shows the secondary current vectors for open-channel flows over smooth-rough bed strips. Figures 1(a) and (b) show simulated results and measured data, respectively, for Wang and Cheng's (2005) experimental case. It can be seen in the figures that the numerical model successfully predicts pairs of counter-rotating secondary flows, i.e., upflows over the smooth strips and downflows over the rough strips. In actual alluvial channels, in which the bed materials are a mixture of well-sorted sediment particles, this type of cellular secondary current sweeps out fine particles over the troughs (rough strips) and transports them onto ridges (smooth strips).

In Figure 1(a), the simulated maximum magnitude of the secondary current vectors appears to be 2.7% of the cross section-averaged velocity. This is very similar to the value of 3% observed in Nezu and Nakagawa's air duct experiment (1984). Note in Figure 1(b) that the velocity vectors near the free surface are larger than those near the bottom, which is contrary to the trends observed in the simulated results in Figures 1(a) and measured data by Muller and Studerus (1979). The larger velocity vectors near the free surface appear to be exaggerated when the *y*-component of velocity vectors (v) is estimated using the continuity relationship.

Figure 2 shows the distribution of the streamwise mean velocity. The simulated result and measured data in Figures 2(a) and (b) are normalized by the depth-averaged velocity at the center of the channel. The figures show that the overall predictions by the numerical model proposed herein are quite successful. It is interesting to note that the isovels are wavy in the transverse direction due to periodic changes in roughness in regions without sidewall effects. That is, in the vicinity of the bottom, the mean velocity over the smooth strip is larger than that over the rough strip. This is, of course, the direct effect of the roughness. On the contrary, in the region away from the bottom, the mean velocity over the rough bed is greater than that over the smooth region.

4. SUSPENDED SEDIMENT TRANSPORT

The transport of suspended sediment in an open-channel flow over smooth-rough bed strips is simulated. It is assumed that suspended particles are uniform with a mean diameter of 80 μ. Therefore, in solving the flow equations, the roughness height of the smooth strips is changed from k_s = 0 μ to k_s = 80 μ to reflect the possible deposition of suspended particles on the smooth bed strips. The computations are based on the decoupled modeling approach between flow and suspended sediment. In addition, the bed elevation change due to deposition of suspended sediment or erosion of the bed is not taken into account.

Figure 3 shows the mean concentration profile for suspended sediment. It can be seen in the figure that the sediment concentration over the smooth strips is higher than that over the rough strips. This is because the rough bed strips are composed of coarser particles that are relatively difficult to be entrained from the bed although the bed shear stress over the rough strips is higher. The contour lines over the smooth strips are bulged towards the free surface, as the result of the upflows in that region. On the contrary, the downflows over the rough strips make the contour lines bulge towards the bottom.

In Figure 4, the transverse distribution of suspended sediment load and depth-averaged streamwise mean velocity simulated by the present numerical model are depicted. It can be seen that the sediment load over the smooth strips is higher than that over the rough strips. This is consistent with field observations by Kinoshita (1967). In the present case, the suspended sediment load is estimated to be 0.012 m^3/s, and about 71% of the total suspended load is carried over the smooth strips. Nezu and Nakagawa (1993) concluded that the downflow region over troughs is characterized by a higher streamwise mean velocity compared with the upflow region over the ridges. However, the simulated results do not show a clear tendency for the mean velocity over the rough strips to be larger. The depth-averaged velocity profile is rather smooth, but shows different trends in dU/dy depending upon the strip type used. That is, dU/dy is negative over the smooth strip located second from the left side wall, while it is positive over the neighboring rough strips. This might be more pronounced if a moving free surface were to be allowed in the computations.

Figure 5 presents the vertical distribution of suspended sediment at various points in the transverse direction. The sediment concentration in the figure is normalized by the near-bed concentration defined by the concentration at a height corresponding to 5% of the flow depth from the bed. The Rousean profile is also provided in the figure for comparison. It can be seen in the

figure that the distribution of suspended sediment is roughly similar depending on the type of the bed. That is, the sediment concentration profile over the smooth strips is more akin to the Rousean distribution compared with that over the rough strips. In contrast, the concentration profiles over the rough strips are more uniform over the depth than the profiles over the smooth strips.

Figure 6 shows the vertical distribution of eddy diffusivity, here, same as eddy viscosity. In the present study, using the simulated results by RSM, eddy viscosity is estimated by

$$\nu_t = C_\mu \frac{k^2}{\varepsilon} \tag{5}$$

where C_μ = 0.09. In the figure, the eddy diffusivity profiles by RSM are compared with profiles obtained from Wang and Cheng (2005). Recognizing the periodicity of variables in the transverse direction for open-channel flows over smooth-rough bed strips, Wang and Cheng (2005) proposed the following relationships for the streamwise mean velocity and Reynolds shear stress:

$$\frac{\kappa \bar{u}(y,z)}{\bar{u}_*} = \left(1+\delta_1 \cos\frac{\pi y}{\lambda}\right)\ln\frac{z}{R_0} + \left(\delta_2 \cos\frac{\pi y}{\lambda}\right)\sin^2\frac{\pi z}{2h} + D\cos\frac{\pi y}{\lambda} \tag{6}$$

$$\frac{\overline{uw}(y,z)}{{u_{*0}}^2} = \left(1+\delta_3 \cos\frac{\pi y}{\lambda}\right)\left(1-\frac{z}{H}\right) + \delta_4 \cos\frac{\pi y}{\lambda}\left(1-\frac{z}{H}\right)\frac{z}{H}\sin\frac{\pi z}{H} \tag{7}$$

where R = zero-velocity level for the logarithmic term, R_0 = zero-velocity level related to base flow, $\bar{u}_*$ = average shear velocity in the central zone, u_{*0} = shear velocity evaluated at the strip edge, and δ_1, δ_2, δ_3, δ_4, D = parameters which can be determined from measured or simulated data. Using these relationships, the eddy viscosity profiles were obtained and are plotted in Figure 6. It can be seen that two profiles from the present model and from Wang and Cheng (2005) are very akin to each other for $z/H < 0.5$. However, for $z/H > 0.5$, the profiles from the numerical simulations appear to be larger than profiles from Wang and Cheng (2005). In the inner region, note that the simulated eddy viscosity over the rough strips is larger than that over the smooth strips. This is due to the higher shear velocity over the rough strips. In the outer region, the secondary currents reverse this situation. That is, the upflows over the smooth strips transport high turbulence near the bottom, whereas the downflows over the rough strips transport low turbulence near the free surface.

5. CONCLUSIONS

In this study, the open-channel flow and suspended sediment transport over smooth-rough bed strips were simulated numerically. The numerical model solved the RANS equations with the Reynolds stress model for turbulence closure. The simulated mean flows were compared with laboratory experiment data reported by Wang and Cheng (2005), showing a good agreement. Using the simulated flow field, the distribution of suspended sediment in such flow was also simulated numerically. The eddy diffusivity concept was used just for simplicity. The simulated results showed that the sediment concentration over smooth strips is higher than over the rough strips. This is consistent with Kinoshita's (1967) field observation. From the numerical simulations, it was also found that the sediment concentration over the smooth strips is quite close to the Rousean distribution, while the concentration over the rough strips is rather uniform over the depth. Finally, the eddy diffusivity profiles were provided. In the region close to the bottom, the eddy diffusivity

over the rough strips is higher, whereas the eddy diffusivity over the smooth strips is higher in the region away from the bottom. This is due to secondary flows or upflows, which transport high turbulent flows from the bottom towards the free surface over the smooth strips.

ACKNOWLEDGEMENTS

A part of the present study was carried out during the first author's sabbatical leave to Ralph M. Parsons Laboratory in MIT. The first author appreciates Dr. Eric Adams, Department of Civil & Environmental Engineering, MIT for his invitation. This research was partly supported by 21st Century Frontier Research Program (code No. 2-3-2 from Sustainable Water Resources Research Center) of the Ministry of Science of Technology in Korea.

REFERENCES

Choi, S.-U. and Kang, H. (2001). "Numerical Tests of Reynolds Stress Closure Models in the Computations of Open-Channel Flows." *The 8th International Symposium on Flow Modeling and Turbulence Measurements*, Tokyo, Japan.

Colombini, M. (1993). "Turbulence-driven secondary flows and formation of sand ridges." *Journal of Fluid Mechanics*, 254, 701-719.

Colombini, M. and Parker, G. (1995). "Longitudinal streaks." *Journal of Fluid Mechanics*, 304, 161-183.

Dietrich, W.E. (1982). "Settling velocity of natural particles." *Water Resource Research*, AGU, 18(6), 1615-1626

Garcia, M. and Parker, G.. (1991). "Entrainment of bed sediment into suspension." *Journal of Hydraulic Engineering*, ASCE, 117(4), 414-435.

Hanjalic, K. and Launder, B.E. (1972). "A Reynolds stress model of turbulence and its application to thin shear flows." *Journal of Fluid Mechanics*, 52, 609-638.

Kinoshita, R. (1967). "An analysis of the movement of flood waters by aerial photography; concerning characteristics of turbulence and surface flow." *Photographic Surveying*, 6, 1-17 (in Japanese).

Lin, C.A. (1990). "Three dimensional computations of injection into swirling cross flow using second moment closure." Ph.D. Thesis, UMIST, Manchester, England.

Mellor, G.L. and Herring, H.J. (1973). "A survey of mean turbulent field closure*." AIAA Journal*, 11, 590-599.

Muller, A. and Studerus, X. (1979). "Secondary flow in an open-channel." *Proc. of 18th IAHR congress*, Cagliari, 3, 19-24.

Naot, D. and Emrani, S. (1983). "Numerical simulation of the hydrodynamic behavior of fuel rod with longitudinal cooling fins." *Nuclear Engineering and Design.*, 73, 319-329.

Naot, D. and Rodi, W. (1982). "Calculation of secondary currents in channel flows." *Journal of the Hydraulic Division*, ASCE, 108(HY8), 948-968.

Nezu, I. and Nakagawa, H. (1984). "Cellular secondary currents in straight conduit." *Journal of Hydraulic Engineering*, ASCE, 110(2), 173-193.

Nezu, I. and Nakagawa, H. (1989). "Self forming mechanism of longitudinal sand ridges and troughs in fluvial open-channel flows." *Proc. of 23rd IAHR congress*, Ottawa, Canada, B65-B72.

Nezu, I. and Nakagawa, H. (1993). *Turbulence in Open-Channel Flows. IAHR Monograph*, Balkema, Rotterdam, The Netherlands.

Nezu, I., Tominaga, A., and Nakagawa, H. (1993). "Field measurements of secondary currents in

straight rivers." *Journal of Hydraulic Engineering*, ASCE, 119(5), 598-614.

Speziale, C.G., Sarkar, S., and Gatski, T. (1991). "Modeling the pressure strain correlation of turbulence: an invariant dynamical systems approach." *Journal of Fluid Mechanics*, 227, 245-272.

Tsjimoto, T. (1989). "Longitudinal stripes of sorting due to cellular secondary currents." *Journal of Hydroscience and Hydraulic Engineering*, 7(1), 14-18.

Vanoni, V.A. (1946). "Transportation of suspended sediment by water." *Transaction of ASCE*, ASCE, 111, 67-133.

Wang, Z.-Q. and Cheng, N.-S. (2005). "Secondary flows over artificial bed strips." *Advances in Water Resources*, 28, 441-450.

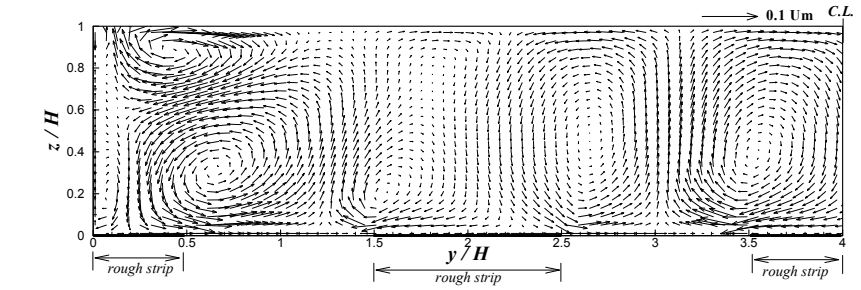

(a) RSM result

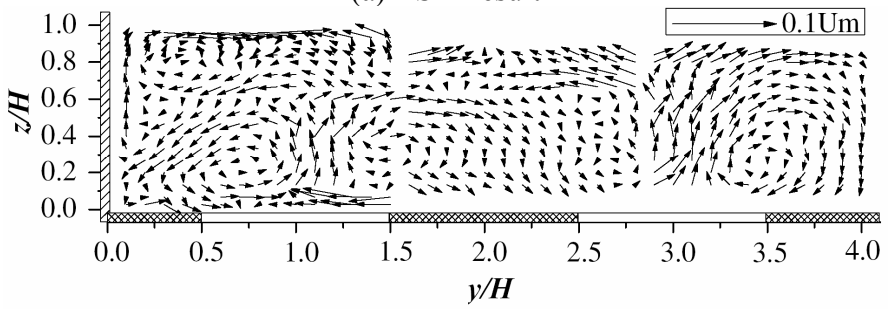

(b) Experimental data by Wang and Cheng (2005)

Figure 1. Cellular Secondary Currents

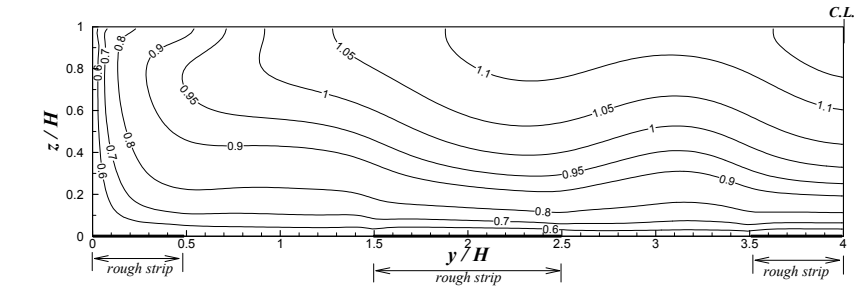

(a) RSM result

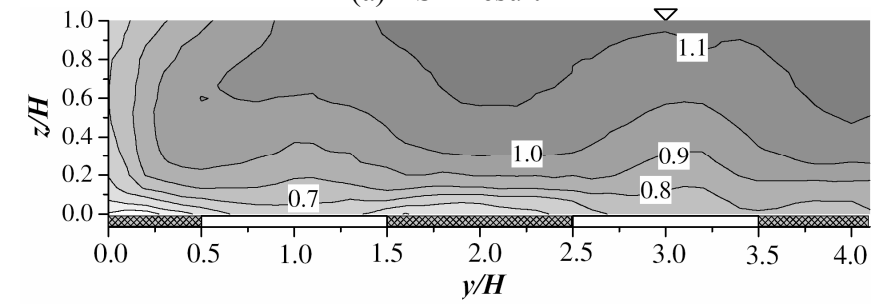

(b) Experimental data by Wang and Cheng (2005)

Figure 2. Contour Plot of Streamwise Mean Velocity ($\bar{u}/U_m$)

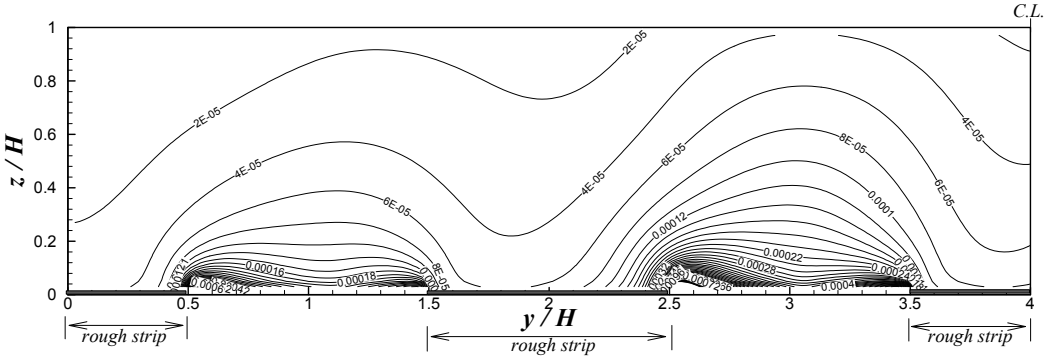

Figure 3. Suspended Sediment Concentration

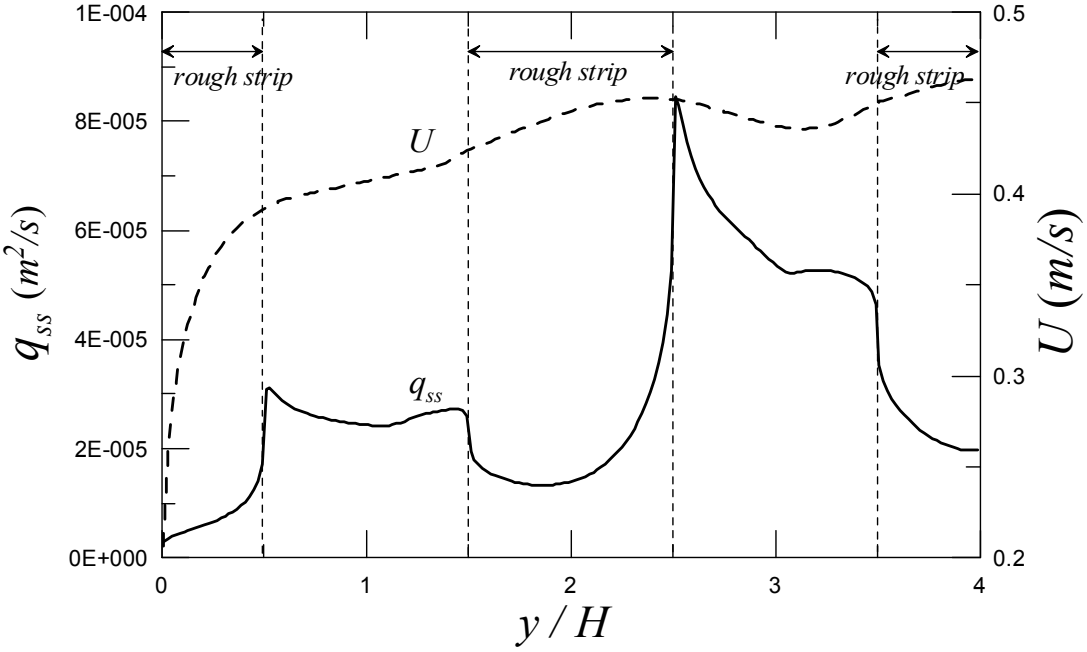

Figure 4. Transverse distributions of suspended sediment load and depth-averaged velocity

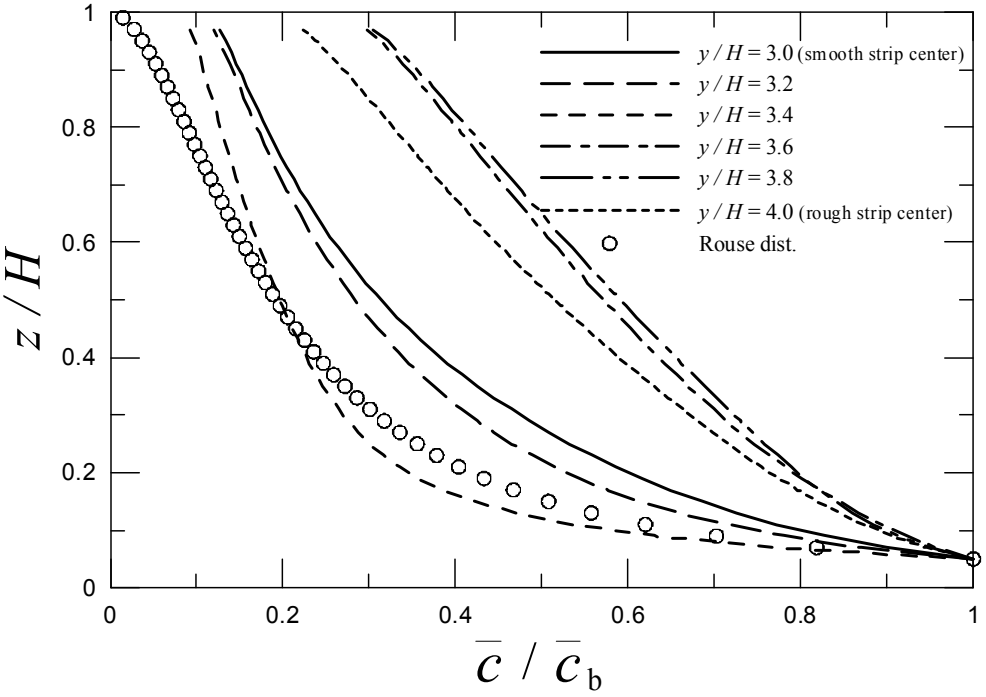

Figure 5. Vertical Distribution of Suspended Sediment

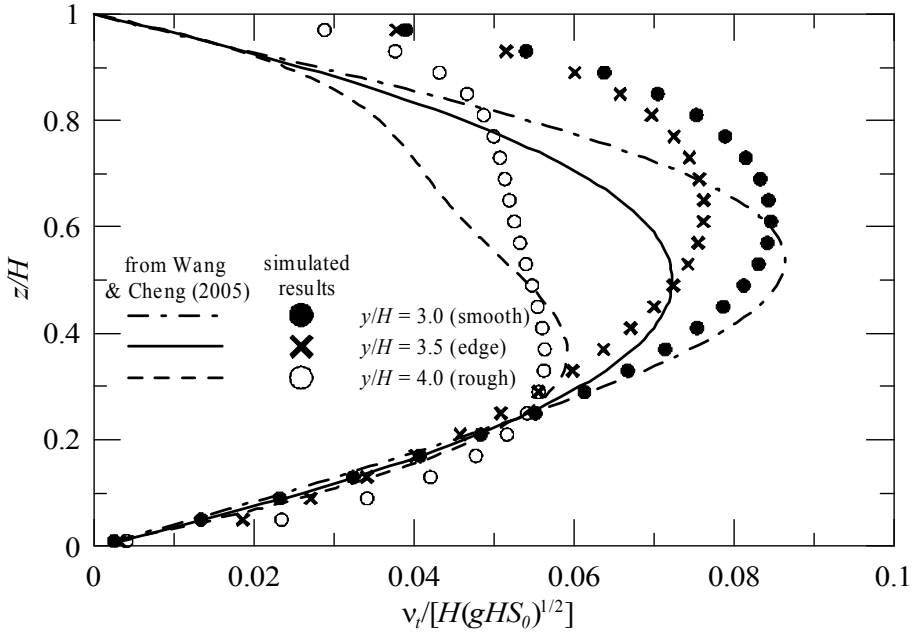

Figure 6. Vertical Distribution of Eddy Viscosity (Eddy Diffusivity)